JOURNAL GEOLOGICAL SOCIETY OF INDIA
Vol.89, January 2017, pp.33-46

# Granitoids of the Magba Shear Zone, West Cameroon, Central Africa: Evidences for Emplacement under Transpressive Tectonic Regime

Benjamin Ntieche[1,2*], M. Ram Mohan[1] and Moundi Amidou[2]

[1]CSIR-National Geophysical Research Institute, Hyderabad - 500 007, India
[2]Department of Earth Sciences, University of Yaounde 1, Cameroon
***E-mail:** ntiechebenjo@yahoo.fr*

## ABSTRACT

**The Magba Shear Zone is made up of granites, migmatites, orthogneiss, metagabbro, mafic dyke and mylonites with coarse grained texture, porphyroblastic, granoblastic, cataclastic and mylonitic texture respectively. Structural features and kinematic indicators testify the syntectonic emplacement of Magba granitoids and also provide detailed information on the relative timing of deformation as follows: (1) D1 of tangential movement immediately followed by (2) the D2 phase which is heterogeneous simple shear in dextral transpressive context with a NW-SE direction (3) D3 tectonic phase is marked by sinistral transpressive tectonic and superposed folding with a NE-SW kinematic direction. Combined ductile NE-SW shear movements and NW-SE compressional movements defined a transpressional tectonic regime during the D3 deformation (4) A brittle stage D4 is controlled by transcurrent tectonics and responsible for the emplacement of faults, and joints. The Magba granites would have intruded along sub-vertical mid-crustal feeder channels and were emplaced as a sheet or sheets along the shear zone during the early stage of the C3 shearing, followed by gabbro and mafic dyke at the late stage. Strike-slip dilatancy pumping under transpressive tectonic is suggested as a possible mechanism for the emplacement of the Magba granites.**

## INTRODUCTION

Magba area is situated at the junction of the Cameroon Central shear zone (CCSZ), the Adamawa fault (AF) and the Tibati-Banyo fault (TBF) in Cameroon (Fig. 1). The CCSZ is a major lineament of the Pan-African orogeny of Central Africa; however the tectonic significance of widespread Pan-African structures at a regional scale is a matter of debate (Ngako et al., 2003; Kankeu et al., 2009). The divergent views include the operation of transpressive tectonics during the Pan-African orogeny in the central Cameroon. Kankeu et al. (2009) have suggested an early convergence and compression ($D_1$) in the eastern Cameroon, followed by further crustal compression with peak metamorphism ($D_2$) and a late Pan-African transpression ($D_3$).

The disposition of Magba area at the junction of shear zones is very important in understanding the CCSZ kinematic deformation regimes, and the emplacement conditions of these rocks. Very few geological investigations have been carried out earlier on the Magba area (Njonfang et al., 2006, 2008; Ntiéche,2009). Hence the current understanding on the petrology and tectonic evolution of the Magba area is very limited. To fill this gap we are presenting herewith detailed structural and petrographic elements for Magba granitoids to provide much insights in understanding the nature of these rocks, their conditions of emplacement and related deformations.

## REGIONAL GEOLOGICAL SETTING

The Precambrian basement complex of Cameroon consists of two major lithostructural units; the Congo craton (CC) and the Central African fold belt (CAFB) (Fig. 1). These rocks record the crustal evolution of the region from the Mesoarchaean to Neoproterozoic (Toteu et al., 1994, 2001). The CAFB is defined by a system of NE-trending faults comprising Tchollire-Banyo fault (TBF), Adamawa fault (AF), Sanaga fault (SF) and Kribi-Campo fault (KCF).

### *The Congo Craton (CC)*

The CC includes a well-preserved Archaean (Ntem Complex) and Palaeoproterozoic domains (Nyong Series) recording the Precambrian crust formation history of Cameroon (Toteu et al., 1994; Basseka et al., 2011). The Ntem Complex is predominantly made of Archaean rocks (3.1–2.5 Ga) that were partially reworked during the Palaeoproterozoic Trans-amazonian cycle (Toteu et al., 1994; Tchameni et al., 2001; Tanko Njiosseu et al., 2005; Shang et al., 2007; Van Schmus et al., 2008). Greenstone belts though volumetrically less, form important litho units within this complex, and show intrusive relationships with the basement rocks. The Archaean basement rocks include high grade charnockites and undifferentiated tonalite–trondhjemite–granite (TTG) suite of rocks (Nédélec et al., 1990; Toteu et al., 1994; Shanget al., 2004, 2007). The Palaeoproterozoic Nyong Series crops out to the west and east of the Ntem Complex (Fig 1; Suh et al., 2008). It is part of the Palaeoproterozoic Trans-amazonian belt, which extends from Central Africa to northeastern Brazil (Toteu et al., 1994; Feybesse et al., 1998; Penaye et al., 2004; Lerouge et al., 2006). The Nyong Series consist mainly of high-grade gneissic rocks, including biotite-hornblende gneiss, charnockite, garnet-amphibole-pyroxenite and Banded Iron Formation (BIF). Pan-African intrusives cut across the Nyong Series rocks and include weakly metamorphosed diorite, granodiorite and syenite, in addition to post-tectonic dolerites at few locations (Toteu et al., 1994; Lerouge et al., 2006).

### *The Central African Fold Belt (CAFB)*

The ~600 ± 70 Ma CAFB is a major collisional belt that underlies the region from the west African Craton to East Africa (Toteu et al., 2006b; Van Schmus et al., 2008). It extends in parts of Nigeria, Cameroon, Chad, Central African Republic and Sudan to Uganda in further east (Toteu et al., 2006b). According to their age, three lithological domains have been identified in the CAFB in Cameroon, namely the Adamawa–Yadé (AYD), Yaoundé and Northwestern Cameroon domains (Toteu et al., 2004; Van Schmus et al., 2008)

The Adamawa-Yade Domain (Toteu et al., 2004; Van Schmus et al., 2008) is the largest domain of the CAFB in Cameroon, dominated by 640–610 Ma, syn- to late-collisional high-K calc-alkaline granitoids (Fig.1). These granitoids intrude high-grade gneisses that represent a Palaeoproterozoic basement, which was likely dismembered during

0016-7622/2017-89-1-33/$ 1.00 

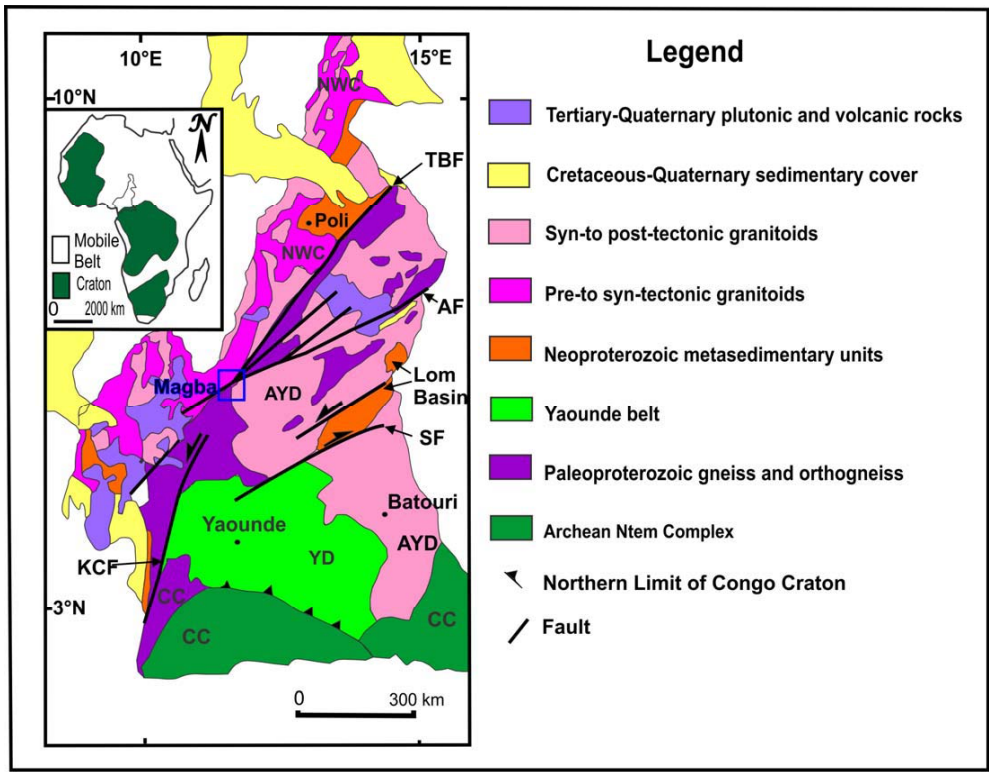


**Fig. 1**. Geological map of Cameroon modified after Toteu et al. (2001). The Central African Shear Zone is defined by a system of NE-trending faults comprising Tchollire-Banyo Fault (TBF), Adamawa Fault (AF), Sanaga Fault (SF), and Kribi-Campo Fault (KCF). The inset is the map of the African continent, showing the location of Cameroon relative to the distribution of cratons and mobile belts.

the Pan-African assembly of western Gondwanaland (Toteu et al., 2004; Tanko Njiosseu et al., 2005; Van Schmus et al., 2008). Toteu et al. (2004, 2006a) classified the rocks of the AYD into three main groups, viz. (a) Large supracrustal blocks of Palaeoproterozoic metasedimentary rocks and orthogneisses with assimilated Archaean crust similar to the Ntem Complex, (b) 612–600 Ma, low- to medium-grade metasedimentary and metavolcaniclastic rocks, and (c) 640–610 Ma syn- to late-tectonic granitoids of transitional composition and crustal origin (Van Schmus et al., 2008).

The Yaoundé Domain consists of an extensive tectonic nappe that was thrusted onto the CC during the Pan-African collision (Nzenti et al., 1988; Toteu et al., 1994, 2004; Van Schmus et al., 2008). This domain is analogous to the Gbayas and Sergipano nappes in central African Republic and Brazil, respectively. Thrust slices of meta-sedimentary rocks with poorly constrained ages of ~626 Ma (Toteu et al., 2006a) are common in the Yaoundé Domain (Van Schmus et al., 2008). Toteu et al. (1994, 2001) suggested that the detrital material was derived from juvenile Palaeoproterozoic and Neoproterozoic sources in the southern part of the AYD, as well as from the Palaeoproterozoic Nyong Series in the CC.

The Northwestern Cameroon Domain is located to the west of the Tcholliré–Banyo fault (TBF), along the western border of Cameroon and extends into eastern Nigeria. It includes a variety of rock types, namely (a) medium- to high-grade schists and gneisses of the ~700 Ma Poli series, (b) ~660–580 Ma calc-alkaline granitoids (diorite, granodiorite, and granite), (c) anorogenic alkaline granitoids, and (d) low-grade sedimentary and volcanic basin sequences (Toteu et al., 2004; Van Schmus et al., 2008). It is generally believed that the CAFB was formed during the Neoproterozoic collision of the West African Craton with the Congo Craton (Toteu et al., 2004). Toteu et al. (2004) proposed a three-phase evolution, which began by the emplacement of calc-alkaline granitic rocks (670–660 Ma), followed by crustal thickening, high-grade metamorphism, calc-alkaline magmatism (640–610 Ma), and finally overprinted by post-collision nappe formation, sub-alkaline to alkaline magmatism (600–545 Ma) and molasse basin sedimentation.

**Geology of Magba Region**

The study area forms part of the Tikary plain, morphologically a transitional zone between the high western plateau and the Adamawa plateau, with an average elevation of 810 m and covers approximately 400 km$^2$ area. It is characterized by two major morphological units namely the plains, made of mylonites and metagabbro and the hills, made of granites, mylonites and migmatites (Ntiéche, 2009). The hills are elongated and oriented N40-45° E (Fig. 2), the orientation being parallel to that of the Cameroon Volcanic Line (Moreau et al., 1987; Njonfang et al., 2006). The rock exposures are limited and confined to slopes and hilltops in lowlands and river beds. These rocks form part of the CCSZ and consist of migmatites, orthogneiss, mylonites, metagabbros and mafic dykes. Mylonites and ganites have cross-cutting relationships with the intrusive younger mafic dykes and quartzo-feldspahic veins while orthogneisses and migmatites are intruded by amphibolitic enclaves. Compositional banding is noticed all through the migmatites, and characterized by (1) gneissosity with good compositional layering with the intrusions of aplite and pegmatite veins; and (2) a metatexitic banding marked by vein injections sub-parallel to the gneissic foliation, the whole unit is being stretched and reinforced by quartzo-feldspathic veins. Folded amphibolitic boudins

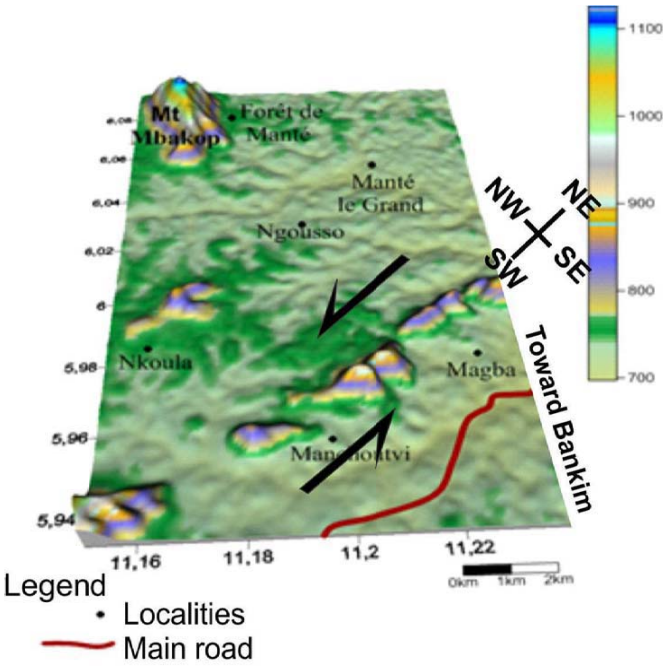


**Fig. 2.** Digital Model Elevation (DME) of the study area showing the alignment of hills (NE-SW).

are observed in the orthogneisses and migmatites, while the faults are mostly confined to mylonites.

## METHODOLOGY

### *Field methods*

Geological fieldwork involved mapping and sample collection. Forty samples were collected, representing various lithologies of the study area. The structural elements (folds, foliations, faults, shears, and lineation) of each tectonic event were documented wherever possible, and their orientation (strike and dip) was measured to relate with regional deformational events that define the structure and emplacement of the granitoids. Geometric analysis of the structural elements was also carried out. It consist of the determination and measurement of structural elements (folds axes, their vergence, strike and dip; fault direction, and vergence, foliation strike and dip).

### *Laboratory methods*

Structural analyses and petrographical studies were performed respectively by using StereoNett software for statistical analyses and by studying thin sections under the microscope. To get an overall orientation of the foliations, schistosity and fractures, the poles of these planes have been plotted in lower hemisphere Schmidt diagrams using conventional techniques (Ragan, 1973). The deformation history and kinematic analysis of the whole area were deduced from the field measurements and detailed studies of foliation and lineation trajectories in addition to observation of meso-to-microscopic criteria of coaxial or non-coaxial strain (e.g. symmetry or asymmetry of shear bands, tails around porphyro clasts, folds).

## FIELD DESCRIPTIONS

The distribution and disposition of different litho units of the Magba area are shown in the geological map (Fig. 3). The description of major litho-units, namely the granites, orthogneisses, migmatites, metagabbro, mafic dykes and mylonites are discussed here.

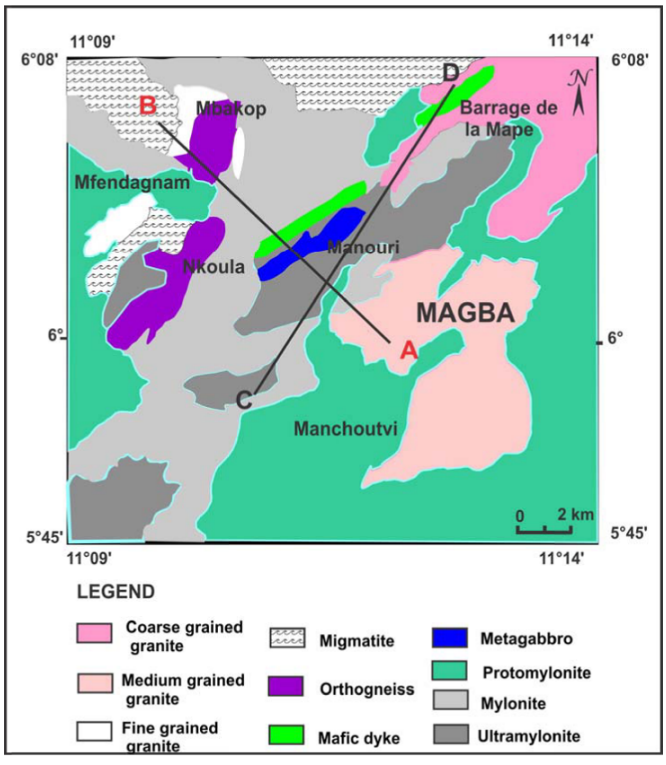


**Fig. 3.** Geological sketch map of the study area.

### *Granites*

Depending on the grain size, granites are divided into coarse, medium and fine grained. Coarse grained granites outcrops are well exposed on the beds of Mape river and dam. They are massive and gray in colour, made of feldspar phenocryst (4 cm× 2 cm) and quartz (1 cm × 0.5 cm) molded by biotite and amphibole flakes. Granites are intruded by mafic dyke oriented in NE-SW (Fig. 4a) of about ten meters long and over fifteen centimeters wide. Thin secondary quartz and epidote veins (3 to 6 meters long and up to 3 cm wide with massive form and greenish to dark colour) cross-cut the outcrop, this could be a local deformation feature.

Medium-grained granites are located on the stream bed of Mape river at the bridge level on Magba-Bankim road and the outcrops are exposed in the slab form (400 m long and 100 m wide). These rocks are massive, and at outcrop scale display pink colour due to the abundance of potassium feldspar crystals. In Magba area, these rocks are gray in colour, made of plagioclase phenocrysts, occur as relics in mylonitized host rocks.

Coarse-to-medium grained granites show magmatic stage pre-full crystallization fabric (pfc) and also solid-state deformation fabric. The magmatic stage fabric is defined either by the randomly oriented euhedral and subhedral feldspar phenocrysts or by an average sub-parallel alignment of the K-feldspar megacrysts in the less deformed granite. The mylonitic foliation (Sm), defined mainly by the preferential alignment of feldspar augen, ribbons of quartz, biotite and sericite streams, are sub-parallel to the magmatic stage deformation fabric.

Fine-grained granites occur as leucocratic at Mfendagnam and hololeucocratic at Mbakop (Fig. 4b), often cross-cut by quartzo-feldspathic veins. Essential minerals are millimeter sized quartz and feldspar. In Mfendagnam, the leucocratic fine grained granites occur in the dauphin back form (Fig. 4c) and shark up to 1.5 m high, 8 m long and 2 m wide.

### *Orthogneiss*

These rocks are exposed in the areas Mbakop, Nkoula, Mfendangam and Mape dam. In Mbacop, orthogneisses are confined to the slopes of the MbaKop hill and occur in the form of ball and slab (6 m long and 4 m wide). Biotite flakes, feldspar and quartz crystals are found in the dark matrix. Magmatic flow is evidenced by the alignment of feldspars and quartz crystals. In Nkoula and Mfendagnam areas, the foliation is defined by alternating dark mafic and clear quartzo-feldspthic bands. Feldspar and quartz minerals are millimeter size (2mm × 1mm) and well aligned in preferential direction.

"σ" porphyroblasts of feldspar are common in Mfendagnam migmatites. Amphibolite intrusions are seen on a local scale in few outcrops (Fig. 4d). In Mape dam area, the foliation is defined by alternating dark bands composed of ferromagnesian minerals and clear quartzo-feldspathic bands. The biotite lamellae (1 mm × 0.5 mm) are observed in the dark bands. At places, migmatisation features are marked by the combination of granitic and gneissic components along with amphibolite intrusions.

### *Migmatites*

Migmatitic outcrops are noticed in Mbakop, Mape dam and Chissa hill areas. In general, migmatites mark the passage of high-temperature metamorphic rocks to crustal igneous rocks. They result from the mineralogical reorganization by insitu partial melting of pre-existing rocks or granitic liquid injection in fractures.

In Mbakop area, these rocks are foliated, leucocratic and marked by a compositional banding characterized by alternating bands of gneisses and amphibolites (Fig.9a). Later intrusions that are broadly parallel to the gneissic foliation are aplite and pegmatite veins and a metatexitic banding marked by vein injections. The migmatitic rock is also made of a light-coloured mobilizate composing quartz and feldspar

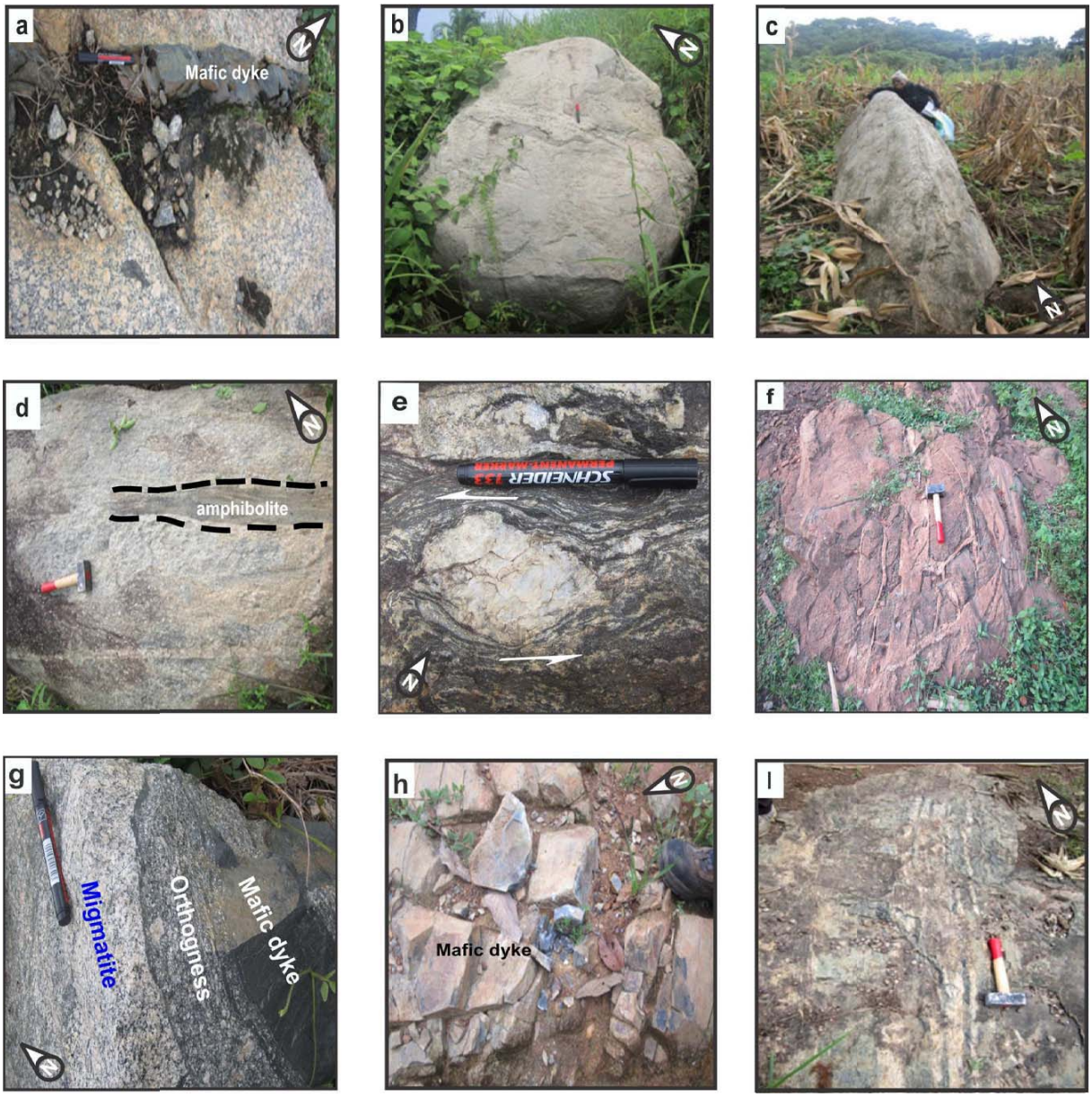


**Fig. 4.** Field photographs of rock types in the study area. **(a)** Coarse grained granite outcrop with mafic vein in Mape dam. Note euhedral K-feldspar megacrysts in granite. **(b)** Hololeucocratic granitic outcrop in Mbakop. **(c)** Fine grained granite outcropping in the form of the back of dauphin in Mfedagnam. **(d)** Orthogneiss in Mfendgnam showing amphibolite intrusion and aligned k-feldspar porphyroblasts. **(e)** Migmatite with feldspar porphyroblast presenting recrystallization tail: note the sinistral sense of shear given by the porphyroblast. **(f)** Metagabbro outcrop presenting feldspar vein system in the form of a spider web. **(g)** Association of migmatite, orthogneiss and mafic dyke. **(h)** Mafic dyke outcrop in Mfembalou with NW-SE and NE-SW fracture directions. **(i)** Ultramylonite outcrop with alternate clear (quartzofeldspathic) and dark (mafic) band in Magba.

which could be the melt product, and of a restitic component constituting biotite, hornblende and pyroxene. The rock unit appears to be stretched and remobilised by quartzo-feldspathic components. These observations suggest that Mbakop migmatites are probable diatexites because of their heterogeneous appearance with the preponderant neosome (molten portion) in relation to paleosome (unmelted portion). The rock is also traversed by quartzo-feldspathic pegmatite vein probably of granitic origin. Imbricated amphibolite boudins are also observed (Figs. 9b and 9d).

In Mape dam, the migmatites are foliated, melanocratic, found in association with the othogneisses, marked by the presence of large crystals of feldspar (10 cm × 6 cm) injected into the gneissic unit during the partial melting of the parent amphibolite, then molded and guided by mafic minerals during deformation. Hence these feldspar crystals have a recrystallization tail and show the sinistral sense of shear (Fig. 4e). Biotite occurs in the form of lamellae (1 cm × 0.5 cm) and confined to the dark portion that constitutes restite. Quartz occurs as fine grained (0.8 cm × 0.6 cm) within the melanocratic frame. All these features suggest that Mape migmatites are metatexitic. The migmatites of Chissa hill area are mainly dark, melanocratic and marked by intense folding of leucosomes.

***Metagabbro***

In Manouri area the metagabbro outcrops are noted in 100 m long over 30 m wide area. The rock is dark greenish in colour and highly banded, having several fractures oriented in different directions and intersecting the sub-vertical mylonitic foliation. The rock is traversed by quartzo-feldspathic veins of varying thickness (1 cm to 20 cm) parallel to the NE-SW banding direction. NE-SW trending prominent sub-vertical stretching lineation defined by elongated feldspar grains

on the foliation plane is recorded. Veins that host feldspar crystals are also molded by melted feldspar matrix. Joints (1 cm to 20 cm thickness) host molded feldspar porphyroblasts in the thin matrix of microcrystals of the same mineral. In places there is a feldspar vein system in the form of a spider web around the centimetric to decimetric block of gabbro (Fig. 4f). Outcrops exhibit dome and basin structures which demonstrate lateral constraints.

***Mafic dykes***

The mafic dykes are exposed in Mape dam and Mfembalouh area on Magba-Mbakop road. In Mape dam area, they occur as NE-SW intrusions of 10m long and 15 cm width. The rock is massive with aphyric texture and intrudes the granite outcrop (Fig. 4a). In some places mafic veins are associated with migmatites and orthogneiss (Fig. 4g). In Mfembalouh, these rocks are massive, oriented in NE-SW direction, occur in relatively wider extent (30 m long and 10 m wide) and is highly fractured, mainly in the NW-SE and NE-SW directions, forming a kind of grid system (Fig. 4h).

***Mylonites***

Mylonites are well distributed in the study area, along the NE and SE of Magba hill, in Manouri, Nkoula areas and Chissa hill. Depending on the extent of deformation, and subsequent retention of the parent rock (granite), the mylonites are divided into three groups: protomylonites (protolith proportion ≥ 50%), mylonites (10% ≤ protolith proportion ≥ 50%), and ultramylonites (protolith proportion ≤ 10%). Protomylonites and mylonites are noticed in Magba hill, Chissa hill, Mfendagnam, and Mbakop areas while the ultramylonites are noticed in Magba and Chissa hill areas.

In Magba area, the protomylonites occur as massive slabs, with feldspars and quartz as major minerals that constitute the rock. Thin secondary veins filled with epidote and/ or chlorites are noticed traversing in all directions, while at some places the quartzo-feldspathic veins are observed intersecting the mylonitic foliation. Few mafic material injections (amphibolite) of varying thickness (3-10 cm) traverse parallel to the foliation. Depending on cross-cutting chronology, mafic injections could be older than quartzo-feldspathic veins. In NE of Magba hill area, the mylonites have similar behaviour as the earlier outcrops described, except that at local scale, magmatic quartzo-feldspathic injections (~0.5 m thick) are noticed containing large feldspar porphyoclasts oriented perpendicular to the mylonitic foliation. At Mfendagnam area, the rock still retains few probable protholithic structures such as aligned feldspar and quartz porhyroclasts reoriented along the mylonitic foliation and the lack of rounded corners and lack of deformation in a very reduced matrix. The clasts exhibit recrystallization tails of "σ" shape symptomatic of a sinistral shearing movement. The outcrop is traversed by quartz veins sub-parallel to the low amplitude mylonitic foliation. At Chissa hill area, the mylonites are locally traversed by quartzo-feldspathic veins that are variably folded.

Ultramylonites are well exposed at the NE and SE of Magba hill, Nkoup river bed and Chissa hill, and are distinct from other rock types of the study area due to the pronounced enrichment of chlorite. Feldspar porphyroclasts are fewer and have rounded to elliptical shape, sparsely occur in a very fine groundmass composed of quartz, feldspar and micas. Intense mylonitic foliation (Sm), defined by sub-parallel alignment of biotite and quartz ribbons in the matrix, give rise to sub-parallel dark and clear bands enriched and devoid of biotite respectively (Fig. 4i). Stair stepping of the feldspar porphyroclasts with their long axis at an acute angle with the mylonitic foliation, together with strike-slip sheared quartzo-feldspathic veins indicates a sinistral sense of shear movement of the rock. Ultramylonite zones display extreme grain size reduction and near absence of visible feldspar porphyroclasts and neocrystallisation of chlorite and sericite transformed the rock into foliated quartz-chlorite rock or phyllonite. The different sub-zones comprising protomylonite, mylonite and ultramylonite within the sheared granite corresponds to the progressive increase in strain, as evident from grain size reduction, progressive disappearance of feldspar porphyroclasts and generation of sericite mica and chlorite, decrease in angle between the S- and C- planes and increasing aspect ratios of the quartz ribbons. Heterogeneous deformation greatly modified the grain size and texture of the rock within Magba shear zone.

**PETROGRAPHY**

Petrography of major lithologies recorded in the area, namely granite, orthogneiss, migmatites, metagabbro, mafic dykes and mylonites are given below.

***Granites***

The granites are coarse to fine-grained and predominantly porphyritic in nature (Figs. 5a and 5b). They are composed of quartz (28%), orthoclase (15%), plagioclase (10%), pyroxene (8 %), biotite (7%), amphibole (5%), microcline (5%) and muscovite (3%) as principal minerals, while allanite (4%), sphene (2%), apatite (2%), epidote (2%) and opaques (1 %) are the accessory minerals. Secondary minerals are represented by myrmekite (2%), chlorite (1%), sericite (3%) and perthite (2%). Quartz is in the form of polycrystalline ribbons of varying size having gears and grain boundary migration (Fig.5b). Quartz grains occasionally react with plagioclase to form myrmekites at the grain boundaries (Fig. 5c).

Plagioclase crystals are sub-euhedral and exhibit albite twins. Some crystals underwent sericitization while orthoclase crystals underwent perthitization reactions (Fig.5d). Pyroxene is in the form of sub-euhedral, moderately elongated phenocrysts. Amphibole is represented by the green hornblende, occur in the sheet form. It contains sphene inclusions and associated with biotites and pyroxenes. Biotites occur as elongated fine fibres, mostly transformed into chlorite. Some biotite fibres contain opaque inclusions while others are resorbed by quartz. Sphene is in the form of columnar rod or sub-rounded form showing characteristic twins.

***Orthogneiss***

Textures of orthogneisses include porhyroblastic, granoblastic (Fig. 5e) and lepidoblastic. The major minerals are quartz (30%), plagioclase (20%), orthoclase (15%), pyroxene (12%), and amphibole (12%). Chlorite (8%) is secondary mineral while sphene (2%) and epidote (1%) are accessory minerals. Quartz is more abundant in the rock and is in the form of polycrystalline ribbons composed of both porphyroblasts and microblasts. Elongated ribbons of quartz show the evidence for dynamic recrystallisation in the form of development of sub-grains, rotation and recrystallization (Fig. 5f).

Quartz porphyroblasts are abundant in Mape dam orthogneiss while quartz microblasts filling the mineral interstices and cracks are observed in the orthogneisses of Mbakop area. Quartz is also present in the form of elongated fibers forming the pressure fringe around the pyrite sub-rounded mineral. Plagioclase is in the form of sub-hedral crystals generally molded by biotite and chlorite. At places plagioclase crystals present as displaced grain fragment or micro fault and curved shapes while others display zoning. Biotite is in the form of flake and fibers with more or less frayed edge. Locally biotite is transformed into chlorite. Amphibole (green hornblende) is anhedral or sub-hedral, flaky sometimes occurs in the form of "amphibole fish". Orthoclase is less abundant in the rock and occurs as large sub-euhedral and anhedral crystals with carlsbad twins, often display cracks filled with biotite. Pyroxenes occur in clusters in Mape dam orthogneisses, as diamond-shaped, while in Mbakop orthogneisses, they occur as twinned or zoned crystals (Fig. 6a). Sphene is very rare in Mape dam

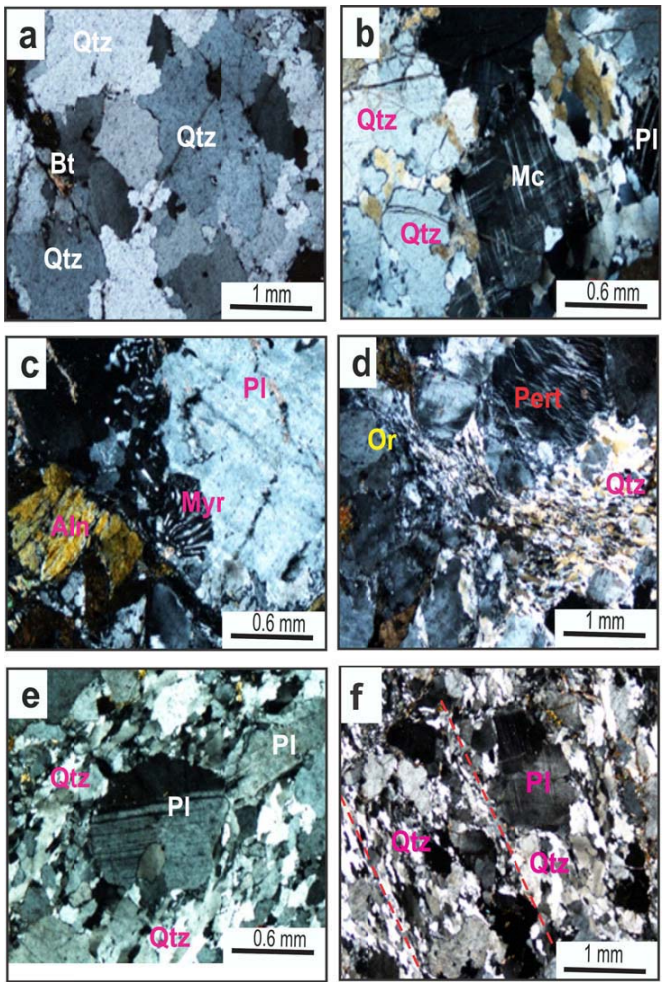


**Fig. 5.** Photomicrographs of rock textures and mineral reactions (Cross Polarized Light). **(a)** Coarse grained texture in granite presenting tiled and imbricated quartz phenocrysts. **(b)** Quartz presenting gears and grain boundary migration. These are evidence for dynamic recrystallization by grain boundary migration. **(c)** Myrmekitic texture marked by intergrowth of quartz crystal on plagioclase in dilational sites ("pressure shadows") around K-feldspar phenocrysts. **(d)** Perthitization of K-Feldspar. Note also recrystallized stream quartz molding feldspar crystals. **(e)** Grano-lepidoblastiv texture in orthogneiss. Note rotated plagioclase surrounded by recrystallized quartz sub-grains. This rock is part of a suite that is syntectonic with a major deformation event. The shape, fabric and the intracrystalline deformation features can therefore be interpreted as sub-magmatic. **(f)** Typical fabric of dynamically recrystallized quartz formed by sub-grain rotation (SGR) recrystallization. Note also the alignment of recrystallized quartz and feldspar.

orthogneiss, but commonly seen in Mbakop, while acicular epidote is noticed in plagioclase porphyroblasts.

***Migmatites***

Migmatites exhibit grano-porphyroblastic texture. The mineralogy is quartz (40%), biotite (15%), myrmekite (2%), chlorite (8%), plagioclase (25%), apatite (4%), microcline (5%) and opaque (1%). In Mape dam, there are two generations of quartz, the first generation is monocrystalline ribbons having gears with undulatory extinction while the second generation is the product of recrystallization, filled along the interstices between the primary minerals resulting in migmatitic foliation to the rock. Plagioclase occurs as sub-hedral crystals with sub-rounded outline moulded by recrystallized quartz crystals and biotite lamellae. Some crystals are fractured bent and kink structures due to tectonic stresses. Most of the crystals are deformed and contain pressure shadows or recrystallization tails filled by biotite or quartz (Fig. 6b). Biotite molds feldspar and quartz porphyroblasts giving the appearance of spider network. Some flakes are transformed into chlorite (Fig. 6c). Microcline is anhedral and presents slightly curved polysynthetic twins of albite and pericline forming a shimmering fine grid with low to very low relief.

***Metagabbros***

Metagabbros of Magba region exhibit porhyroblastic textures (Fig. 6d) and are made of plagioclase (40%), microcline (15%), orthoclase (8%), pyroxene (5%), amphibole (4%) and biotite (2%) as primary minerals while only sericite (25%) is the secondary mineral and opaque (1%) accessory mineral. Plagioclase crystals are more abundant, sub-euhedral and exhibit polysynthetic twinning. Though very limited, also occur as inclusions in orthoclase. Sericite occur in the form of pasty bands, developed due to sericitization of plagioclase (Fig. 6d). Microcline crystals sometimes contain amphibole inclusions. Orthoclase crystals are less abundant in the rock while pyroxene is in

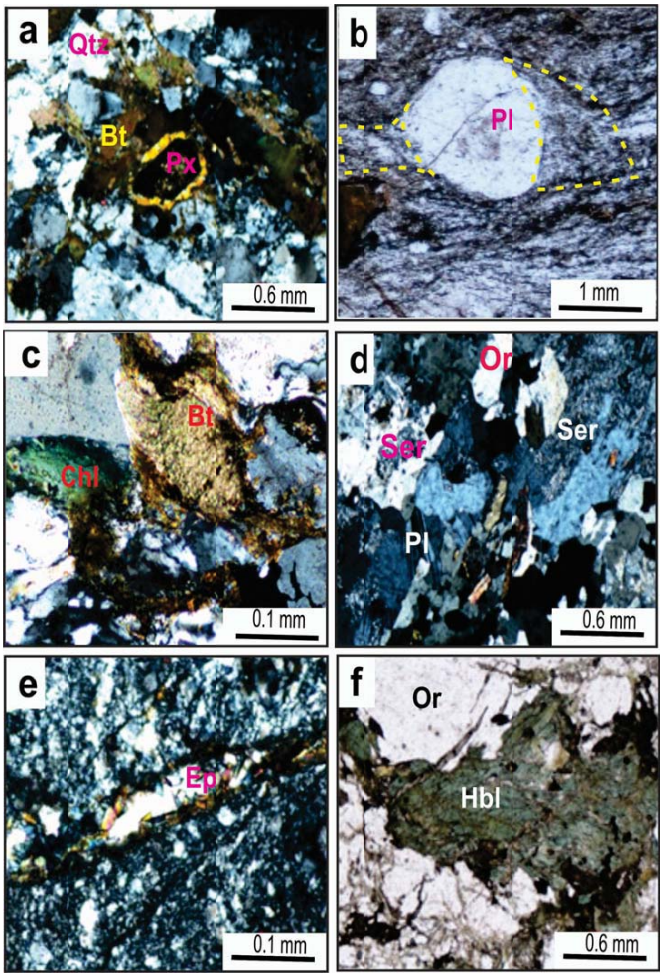


**Fig. 6**. Photomicrographs showing rock textures and mineral reactions. (a, c, d, e = Cross Polarized Light; b and f = Plane Polarized Light). **(a)** Corona texture on altered pyroxene (Px). **(b)** Plagioclase (Pl) porphyroclasts presenting pressure shadow filed by quartz (Qtz) and biotite (Bt). **(c)** Chloritization of biotite (Bt). **(d)** Porphyroblastic texture in metagabbro. Note the sericitazation of plagioclase (Pl). **(e)** Antiaxial epidote (Ep) vein in mafic dykes. Epidote minerals are parallel or perpendicular to the walls of the vein, leaving gap in the center. **(f)** Curved branching amphibole (Hbl) on Mape dam mafic dyke. This shape is exclusively found in mafic dykes.

the form of elongated strips with rectangular sections. Amphiboles are very rare in the rock and occur as thin flakes. Opaque minerals are euhedral sometime with hexagonal form and disseminated in the rock.

***Mafic Dykes***

These rocks exhibit cataclastic textures marked by alternating layers of dark and light coloured minerals. Crushed minerals are indistinguishable microscopically. Some phenocrysts that resisted crushing are visible such as amphibole (30%), orthoclase (25%), chlorite (20%), pyroxene (15%), epidote (6%), zircon (5%) and oxides (4%). Amphibole is represented by the green hornblende and occurs as clusters of curved branching flakes which are a characteristic of Magba dykes (Fig. 6e). Sometimes the amphiboles occur as sub-rounded to sub-hedral crystals, as well as like "amphibole fish" shape suggesting their growth during deformation. Chlorites are the alteration products of amphiboles and they fill the interstices left by previously crystallized minerals. Pyroxenes occur as phenocrysts of uneven square or diamond-shaped. Orthoclase occurs as largely fractured anhedral phenocrysts of variable sizes, includes almond-shaped and "σ" type porphyroclasts, indicating the sinistral sense of shear these rocks had undergone. Few orthoclase crystals also contain amphibole and opaque inclusions. Epidotes occur as euhedral to sub-hedral crystals. In the matrix they are anhedral while in the veins they are particularly in euhedral form, oriented perpendicular to the walls of the vein leaving gap in the center (Fig. 6f). Opaques are less abundant, euhedral to sub-hedral and are found in fractures and mineral interstices. Zircon is the least visible mineral in the rock. It is euhedral with high relief and with halos due to radioactivity.

***Mylonite***

Strain heterogeneity within the Magba shear zone is evident from the development of proto- to ultramylonite zones, with granoclastic (Fig. 7a), ocelar mylonitic (Fig. 7b) and cataclastic textures (Fig. 7c) respectively for protomylonite, mylonite and ultramylonites. Primary minerals are quartz (20%), orthoclase (15%), plagioclase (10%), biotite (8%), amphibole (6%), microcline (5%); secondary minerals are sericite (8%), myrmekite (2%) and chlorite (10%) while zircon (2%), sphene (2%), tourmaline (1%), epidote (1%), apatite (1%), leucoxene (5%) and opaques (4%) are accessory minerals. Pyroxenes are confined to mylonites while amphiboles and microclines are observed in mylonites and ultramylonites. Protomylonites are characterized by weakly developed fabric, defined by the elongated quartz and feldspar grains. Quartz and orthoclase porphyroclasts yield to brittle failure producing fragmented grains and also to crystal plastic deformation resulting in deformation lamellae and grain refinement through recrystallization (Fig. 7d).

Quartz phenocrysts exhibit globular and granular shapes with undulatory extinction and are scattered in the crushed recrystallized matrix while microcrysts forming bands parallel to biotite ("biotite fish") layers giving the rock a curved mylonitic foliation (Fig. 7e). At Mbakop, some biotite flakes are folded and have curved pressure shadow (Fig. 7f). Some quartzofeldspathic layers are folded having S type shape indicating the sinistral sense of shear the rock had undergone (Fig. 8a).

Most of plagioclase and orthoclase porphyroclasts exhibit "σ" or "δ" (Fig. 8b), recrystallization tails and other rolling structures giving the sinistral sense of shear. Highly fractured plagioclases are also present (Fig. 8c). Sericitization is noted only in protomylonites while myrmekitization is observed in protomylonites and mylonites. Perthitic texture is also noted. Feldspar phenocrysts exhibit simple and staircase type displacements (Fig. 8d) and "chevron"/ "kink" type deformation mark by changes in extinction position or changes in the orientation of twin or exsolution lamellae in feldspars (Fig. 8e).

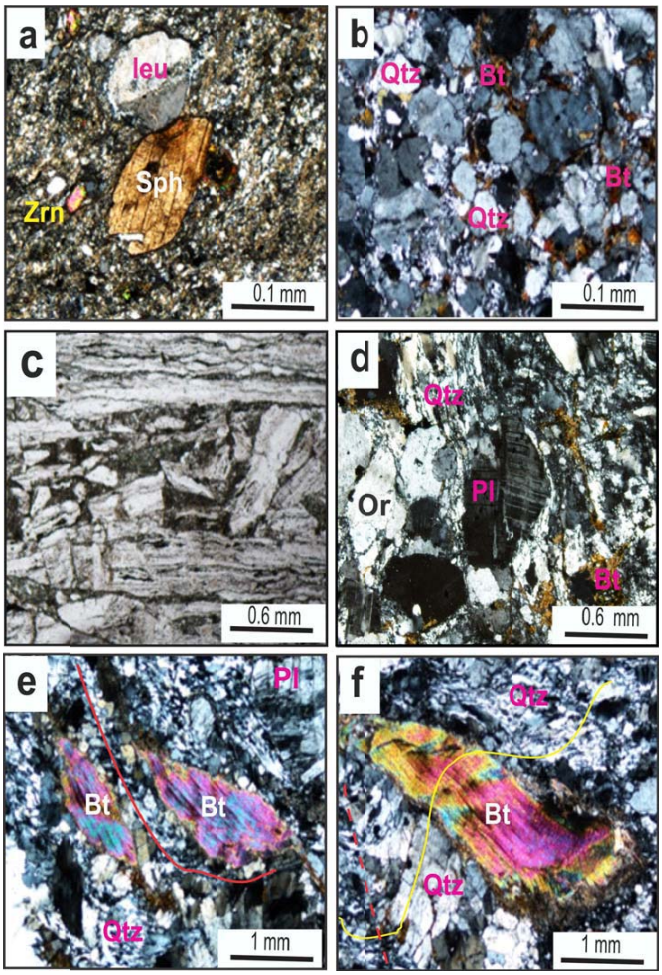


**Fig. 7.** Photomicrographs presenting microstructures and rock textures. (a, b, d, e = Cross Polarized Light; c and f = Plane Polarized Light). **(a)** Granoclastic texture in mylonites. Note totally converted sphene (Sph) into Leucoxene (Leu). **(b)** Ocelar mylonitic texture in protomylonite. **(c)** Cataclastic texture in ultramylonite. **(d)** Deformation lamellae and grain refinement through recrystallization. **(e)** "Mica fish" and quartz (Qtz) mineral alignment describing curved foliation defined by biotite and quartz lying at angle of about 45° to the upper edge of the plate. It curves smoothly to give the sinistral sense of shear to the rock. **(f)** Biotite flake with curved pressure shadow; also notice fold highlighted by the curved (crenulated) foliation defined by rotated aligned quartz.

Amphiboles are represented by green hornblende and glauco-phane. Green hornblende is sub-euhedral and occur as curved tracks associated with biotite, and also as "amphibole fish" (Fig. 8f). Retrograde metamorphism marked by amphibole converting to chlorite is observed at few places. Opaques and zircon inclusions are observed along the margins of biotites, and such inclusions are identified in orthoclase also. Most biotite flakes underwent early chloritization. Leucoxene and tourmaline are euhedral and only found in ultramylonite while apatites are found in protomylonites and mylonites.

## DEFORMATION PHASES

Based on "cross-cutting" relationships (Hancock and Rutland, 1984), macroscopic overprinting relations and microscopic studies, four phases of deformation ($D_1$ to $D_4$) have been identified on Magba granitoids. All the four deformation phases ($D_1$ to $D_4$) are observed in the migmatites, while the granites, mylonites, mafic dykes and metagabbro have recorded only $D_3$ and $D_4$ structures.

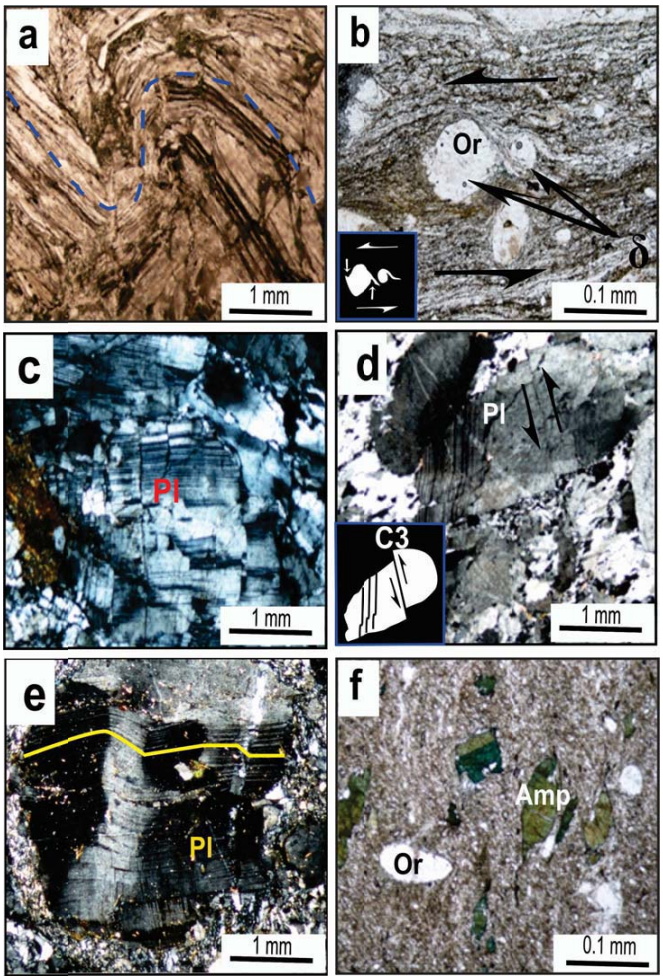


**Fig. 8.** Photomicrographs showing microstructures and kinematic indicators (c, d, e = Cross Polarized Light; a, b, f = Plane Polarized Light). **(a)** "S" type microfold in mylonite presenting the sinistral sense of shear. **(b)** "δ" and "σ" feldspar porphyroclast on ultramylonite. The deflection of the tails around the porphyroclasts shows clearly the sinistral sense of shear. **(c)** Highly fractured plagioclase porphyroclast in mylonite. **(d)** Sinistral strike slip shears ($C_3$) on plagioclase porphyroclast in Magba protomylonite. Also note the curved twins and displaced grain fragments. **(e)** Kink deformation on plagioclase phenocryst. **(f)** "Amphibole fish" on ultramylonite.

### *$D_1$ deformation phase*

The first deformation phase is quite pronounced in nature and is found in migmatite as ($S_1$) foliation or compositional banding outlined by alternating light and dark bands and also fine and coarse-grained granoblastics bands (Fig.9a).The foliation surfaces ($S_1$) have low to moderate dips (0 - 45°) to the ENE and WSW. The poles $S_1$ from the outcrops show a girdle distribution (Fig. 11a),which may imply folding around a gently SSE plunging axis. The associated lineation is a mineral stretching lineation. It trends NNW-SSE with a gentle plunge (0-10°) towards the north, but secondary south plunging lineations are also observed. At places $D_1$ is a relic phase obliterated by the structures in subsequent phases of deformation.

### *$D_2$ deformation phase*

The $D_2$ is characterized by heterogeneous deformation affecting the previous deformation ($D_1$). $D_2$ deformation is associated with the development of ($S_2$) foliation, ($F_2$) folds, the stretching lineation ($L_2$) and boudins ($B_2$) (Fig. 9b).

In Mbakop, asymmetric tight and recumbent ($F_2$) folds mainly overturned towards the SE and asymmetric amphibolite boudins ($B_2$), both indicates the dextral sense of movement (Fig. 9b). Folds ($F_2$) in general are syn-migmatitic, and show wide variation in dip (0 - 30°) resulting in overturned to near recumbent geometry. $S_2$ foliation with axial plane broadly striking NW-SE and low to moderate dips (10 - 40°) predominantly SW is recorded (Fig. 11b). Asymmetry of the folds indicates a consistent eastward vergence. Stretched banding is folded together with the old core section, thereby reflecting the relationship between folding and boudinage (Fig. 9b). Lineation ($L_2$) is characterized by the preferential orientation of feldspar and quartz clasts.

In Chissa hill migmatites, the second deformation ($D_2$) is represented by tight folds ($F_2$) and crenulations schistosity ($S_2$), having a N135° - 160°E direction.

Crenulation cleavage defines new axial plane schistosity in $F_2$ folds (Fig. 9c). The main schistosity in the migmatite is therefore labeled as $S_1/S_2$, which is a composite schistosity. The geometry of folds $F_2$ (short wavelength showing long and short sides) has great significance. It draws the Z in the normal side and S in the opposite side. Asymmetry of those "S" or "Z" folds provides the sense of transport of folded unit toward the east of the outcrop (Fig. 9c). The dip of the axial planes varies from near horizontal to about 60º NW, though they are predominantly gentle easterly dipping. The axial planar dip decreases with increasing tightness and asymmetry of the folds. Dextral movement is the general displacement sense of the $D_2$ deformation.

### *$D_3$ deformation phase*

The third phase of deformation ($D_3$) is well developed in the study area. It is typically a shearing phase and has been recognized in all rock types. The structures associated with this deformation phase are the result of the transposition and redirecting of the $D_2$ structures. It is evidenced by the ($F_3$) folds, shear ($C_3$), boudins ($B_3$) and ($S_3$) mylonitic foliation. ($F_3$) folds are visible on migmatites and leucocratic granites and are marked by tight and lying folds with sub-horizontal hinge on leucocratic frame striking NE-SW. Asymmetric boudins ($B_3$) are found in migmatites and is folded by ($F_3$) fold (Fig. 9d).

New axial plane schistosity is formed on migmatites during the $D_3$ deformation. The mineral lineation $L_3$ is roughly parallel to the gently dipping (0-30°) $F_3$ fold axes and $C_3$ shear plane striking N40°-50°E (Fig. 9d). $S_3$ foliation overprints the pre-existing composite $S_1/S_2$ foliation and trend also NE-SW with moderate to higher dip (2-85°) toward SE (Fig. 11c). "S" type fold ($F_3$) (Fig. 9e) and recumbent ($F_3$) folds (Fig. 9f) present a westward vergence and axial plane plunges eastward. These observations underline the syn or late-$D_3$ status of the sinistral strike slip movement overprinting the dextral shear deformation in rocks along the Magba shear zone. The geometric and kinematic evidences, therefore, indicate an overall NW-SE horizontal compression.

In metagabbro and mylonite shears, are rarely seen while some ($C_3$) sheared fault with sinistral sense of movement are mesoscopically (Fig. 10a) and microscopically (Fig. 10b) observed in Magba ultra-mylonites. In granites and orthogneisses, a penetrative foliation ($S_3$) trending NE-SW is marked by a magmatic flow evidenced by the preferred orientation of potassium feldspar phenocrysts striking in the same direction of the foliation (Fig.10c, Fig. 11d, and Fig. 11e). The foliation is mostly sub-horizontal in mylonites indicating a sheet-like "tongue" structure for the Magba rocks. S-C foliation and "σ" porphyroclast are also present in orthogneiss (Fig. 10d).

In mylonites ($S_3$) foliation is marked by sub-vertical to sub-horizontal alternating discrete quartzo-feldspathic and dark ferro-magnesian layers, striking NE-SW direction (Fig. 11f). In metagabbro, $D_3$ is marked by a NE-SW sub-vertical mylonitic foliation ($S_3$) characterized by alternating dark mafic and clear feldspathic bands

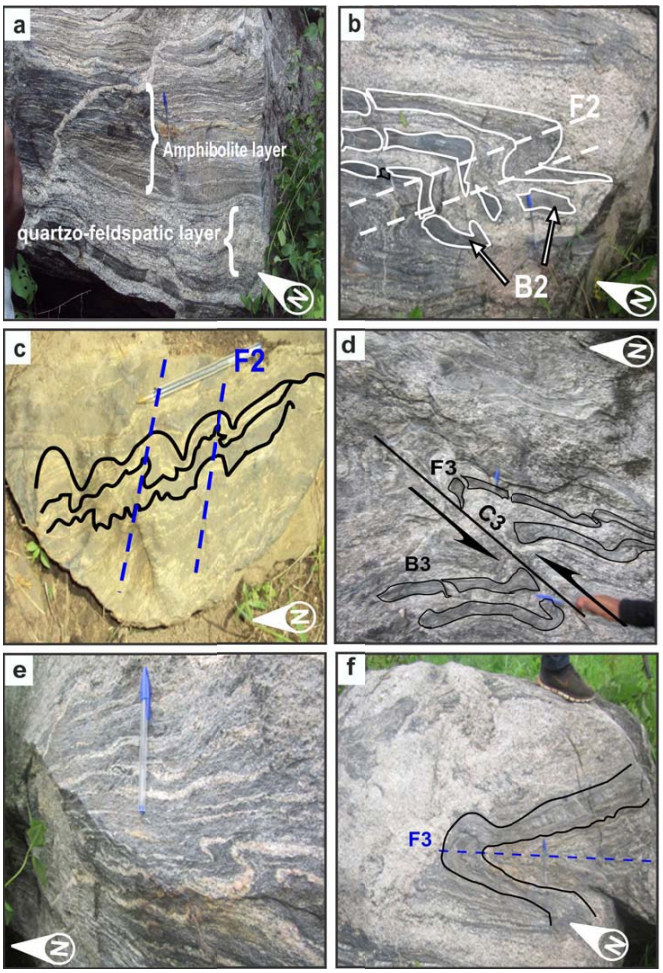


**Fig.9.** Field photographs showing deformation features. **(a)** Foliation ($S_1$) marked by compositional banding in Mbakop migmatites. **(b)** Fold ($F_2$) with Est vergence in Mbakop Migmatite. Note the folded asymmetric boudins ($B_2$) showing the dextral sense of movement to the rock. **(c)** folds ($F_2$) with east vergence on Chissa ultramylonite. Note the dextral sense of shear. **(d)** Shear ($C_3$) and imbricated boudins ($B_3$) with sinistral sense of movement on Mbakop migmatite. **(e)** "S" type folds in Mbakop migmatites presenting also the sinistral sense of movement. **(f)** Lying fold ($F_3$) in Mbakop migmatites. Note the parallelism between the foliation and the axial plane.

(Fig. 10e) and also by feldspar porphyroblast, stretching ($L_3$) lineation striking in the NE-SW direction with (0-15°) NW dip (Fig. 11g).

### *$D_4$ deformation phase*

The fourth phase of deformation ($D_4$) is essentially a brittle phase. It is marked by ($F_4$) faults (Fig. 10f) and ($J_4$) joints. Faults and micro-faults are common in all rock types in Magba area. They are mainly sub-vertical with three main directions E-W, NE-SW and NW-SE (Fig. 11h). Conjugate microscopic and mesoscopic faults striking N00-N10°E; N20-N30°E; and N60-N80°E are present respectively on Mfembalou mafic dyke and Manouri metagabbros. Several dry and filled joints are ubiquitous in Magba rocks.

## KINEMATIC INDICATORS

Several kinematic indicators have been registered in the Magba granitoids. They are σ and δ porphyroblasts, pressure shadows and curved foliation, asymmetric fold, asymmetric boudins, mica and amphibole fish, S-C fabrics, displaced grain fragments, tiled and imbricated porphyroclasts and asymmetric microboudins and microfolds.

### *"σ" and "δ" porphyroclasts*

Ultramylonite of the Mont Chissa area displays two types of porhyroclasts ("σ" and "δ") (Fig. 8b) presenting the rolling structure while Magba ultramylonite presents only the "δ" type. The feldspar porphyroclasts have stair-stepping tails giving a sinistral sense of shear. "σ" porphyroblast is macroscopically recorded in Chissa ultra-mylonites and Nkoula orthogneisses (Fig. 10d) exhibiting sinistral sense of shear.

### *Pressure shadows and fringes*

Magba granitoids display pressure fringes marked by quartz fibres with a constant extinction around the circular pyrite grain at the center suggesting that they have grown along slightly curved trajectories due to rotation. Moreover, pressure shadows are marked in feldspar by recrystallized quartz and biotite filling plagioclase porphyroblast edge (Fig. 6b) and in biotite by curved frayed edge (Fig. 7f).

### *Curved foliation*

Many outcrops in the study area have a foliation that curves smoothly across the shear zone. Microscopically curved foliation is

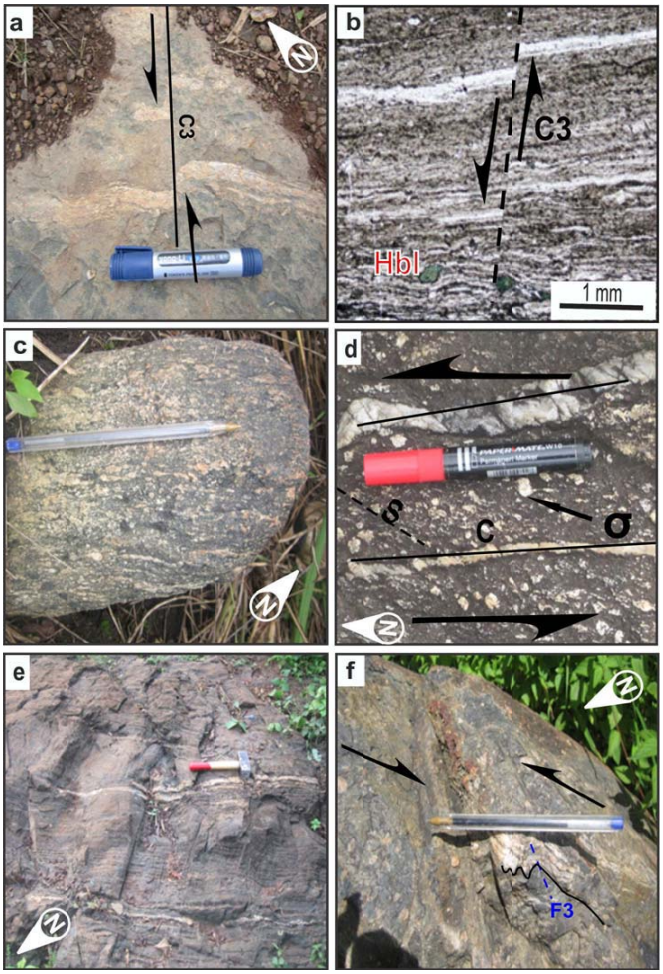


**Fig.10.** Field photographs showing deformation features. **(a)** Sinistral shear ($C_3$) on Magba ultramylonite. **(b)** Sinistral normal sheared fault ($C_3$) in Mfombalou mafic dyke. Note also "σ" shape amphibole porphyroblast. **(c)** Magmatic flow marked by feldspar megacrysts alignment in Mbakop orthogneiss. **(d)** "S-C" structure with mantled "σ" feldspar prophyroblast giving the sinistral sense of shear to Mfendagnam orthogneiss. Note also the alignment of K-feldspar porphyroblasts. **(e)** Banding and fault in Manouri metagabbro. **(f)** Normal fault in ultramylonite.

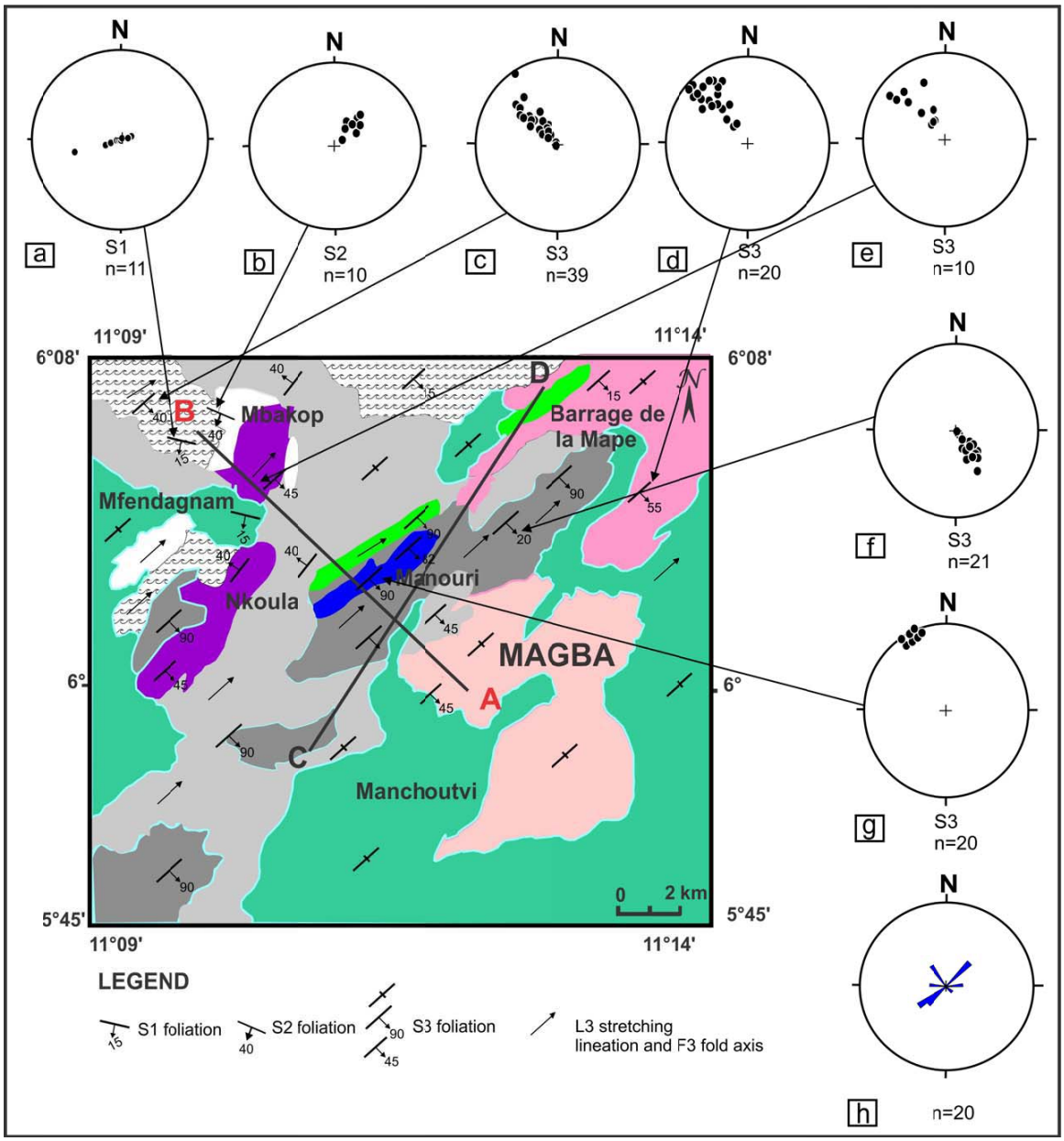


**Fig. 11.** Structural sketch map of the study area and Equal-area Schmidt lower hemisphere projection of structural data: (a), (b) and (c) poles to foliations $S_1$, $S_2$ and $S_3$ respectively on Mbakop migmatites; (d), (e), ( f) and (g) poles to foliations $S_3$ on Mape river granite, Mfendagnam orthogneiss, Magba mylonites, and Manouri Metagabbro respectively. (h) Rose diagram of fracture planes depicting three main structural trends (N80-85E; N30-60E; and N120-140E).

defined in Magba mylonites by mica fish giving the sinistral sense of shear (Fig. 7e). Macroscopically, the rotation of the foliation from the outside to the center of the shear zone is the same as the sinistral shear sense of the overall Magba shear zone.

***Asymmetric fold and microfolds***

A special type of asymmetric fold is generated by the interaction between rigid inclusions and layering. In Mbakop area, two senses of displacement have been recorded. The first one belongs to the second phase of deformation, represented by asymmetric folded amphibolitic layer with east vergence indicating the dextral sense of movement (Fig. 9b) while the second sense of displacement (represented by sheared and imbricated boudins) relates to the third generation of deformation and indicates the sinistral sense of shear with the axial plane parallel to the foliation (Fig. 9d). Magba's ultramylonites also display asymmetric micro fold $F_3$ with "S" shape indicating the sinistral sense of shear (Fig. 8a).

***Asymmetric boudins and microboudins***

Boudins in non-coaxial deformation are asymmetric, due either to modification of initially symmetrical boudins types I and II (Hanmer 1986), or due to the development of asymmetric boudins type III (Goldstein, 1988). At Mbakop area, the type III microboudins are recorded and separated from shears that are inclined to the shear plane. The boudins are displaced in the dextral ($B_2$) (Fig 9b) and a sinistral ($B_3$) sense (Fig 9d). Asymmetric microboudins are also present in Magba ultramylonite.

***Mica and amphibole fish***

Mica fish are a distinctive type of porphyroclast consisting of elongated single crystals of mica, often associated with tails (Lister and Snoke, 1984; Hanmer, 1986; Passchier and Trouw, 1996). In Magba area, the occurrence of mica fish and amphibole fish are noticed. Stair stepping of the tails can be used as a shear sense indicator and the sense of the acute rotation from the long axis of the fish to

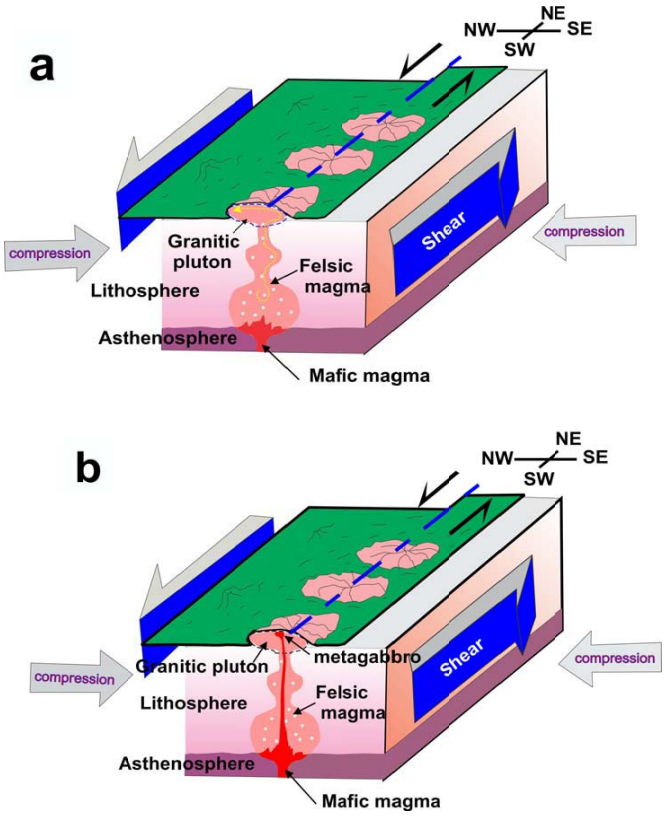


**Fig. 12.** A schematic model for the structure and the emplacement of the Magba granite. **(a)** Early third phase of deformation characterized by the granitic magma injection into active sub-vertical mid-crustal shear zones ($C_3$ shear) operating as feeder channel ways. **(b)** Late third phase of deformation marked by metagabbro and mafic dyke emplacement along shear ($C_3$).

the shear plane also gives the shear sense directly. The formation of mica fish or amphibole fish is not well understood, but may involve development of tails by recrystallization dynamic as well as cataclasis, and rotation of the fish (Blenkinsop, 1989). In Mbakop and Mfembalou area, mica fish (Fig 7e) and amphibole fish (Fig. 8f) indicate sinistral sense of shear.

***S-C fabrics***

S-C fabrics are documented at the mesoscopic (Fig. 10d) and microscopic scales on Nfendagnam orthogneiss and the Mape dam orthogneiss respectively in the form of euhedral little deformed feldspar grains with S- and C-orientations, suggesting that the S-C fabric formed in a sub-magmatic state (Miller and Paterson, 1994).

***Displaced grain fragments, tiled and imbricated phenocrysts***

A small displacement on fault is measured by matching individual grains on either side of the fault in plagioclase. Two generations of displaced grain fragments have been recorded on plagioclase. The first generation is marked by a fracture filled with few crystals of epidote while the second generation displays a dry fracture with a sinistral sense of shear (Fig. 8d). The sub-hedral quartz and feldspar phenocrysts in the Magba granite are frequently imbricated as tiles on a roof (tiling), forming a magmatic lineation in the granite (Fig. 5a). The tiling of phenocrysts indicates non-coaxial deformation in a viscous material and involves rotation of the phenocrysts, and deformation of rock in a magmatic state (Den Tex, 1969; Blumenfeld, 1983; Blumenfeld and Bouchez, 1988; Paterson et al., 1989; Ildefonse et al., 1992a, b).

Other markers of plastic and brittle deformations are recorded in Magba granitoids such as kinking (Fig. 8e), faults and micro cracks.

## DISCUSSION

***Evidence for polyphase deformation and transpressive tectonics on Magba rocks***

$D_1$ deformation phase in the Magba area is related to the initial nappe stacking phase that was emplaced horizontally to form a classical fold-and-thrust belt (Burg et al., 1993). $S_1$ foliation is dipping to the ENE. The nappe vergence in Magba area, deduced from transport direction, is almost similar to that observed in southern domain of the North Equatorial Pan African Belt (Nzenti et al., 1988; Mvondo et al., 2007). $D_1$ fabric has been progressively overprinted by $D_2$ deformation.

The $D_2$ deformation as defined in this study is characterized by recumbent folds with SE vergence. The recumbent folds ($F_2$) along with specific layers indicate thrusting towards the SE during the $D_2$ deformation.

Mineral and stretching lineations are oriented towards the fold axis, suggesting that simple shear caused the folding. Lineation fabric gently plunging primarily towards the NW, and secondarily towards SE, are consistent with predominance of directional to gently oblique movements. Planar and linear data relationships are also coherent with oblique displacements.

The $D_3$ phase is fundamentally a phase of tectonic superposition. It is essentially made of $F_3$ folds resulting in the refolding of the $F_2$ folds. $C_3$ shear is also well represented. The other structures acquired during this phase ($S_3$ schistosity or foliation, $L_3$ lineation) are the outcome of the redistribution or reorganization of their equivalent during the $D_2$ phase, in the sense that some remain parallel and others subparallel or oblique. Transpressive character of deformation during this phase is evident by the coexistence of transcurrent and compressive structures and the parallelism of fold axis and lineation. Magba granitoid structures testify a change in kinematic direction from NW–SE dextral transpressive ($D_2$) to NE–SW sinistral transpressive ($D_3$) phases during the development of the shear zone. The dextral shearing event was thereafter followed by the reactivation of the NE-SW sinistral fault. The observed deformation chronology is different to that of Ngako et al. ( 2003, 2008) and also to that of Tcheumenak et al. (2014) who had documented an initial sinistral movement ($D_2$) followed by a dextral shear movement ($D_3$) along the Cameroon Central Shear Zone and the Fodjomekwet-Fotouni shear zone respectively, in the western part of CCSZ.

The linear megastructure shows horizontal compression and the distribution of associated sinistral structures, suggest that the whole fault system in Magba area represents a sinistral shear zone. The overturned, asymmetric geometry of the folds ($F_3$) with their consistent eastward dipping axial planes with variable dips, westward vergence together with sub-horizontal disposition of the longer limb indicate non-coaxial (shear related) deformation and transportation of the litho units from east to west along the MSZ implying a thick-skinned (tectonic) thrusting. The orientations of ($F_3$) axial planes along NE-SW direction with steep dips are suggestive of a NW-SE compressional tectonic regime during the $D_3$ deformation.

The coexistence of folding and shearing in the Magba area can be interpreted as the effect of deformation partitioning at mid-crustal depths (Bell, 1981; Dabo et al., 2008). Earlier studies have demonstrated that one of the specific consequences of transpression is the partitioning of strain into domains that are predominantly transcurrent associated with domains that are predominantly compressive (Cobbold et al., 1991; Jones and Tanner, 1997; Tikoff and de Saint Blanquatt, 1997).

$D_4$ is a phase of brittle deformation with sub-vertical fractures and regional–scale faults. These fractures are developed in three main directions, mostly in accordance with the main orientations of the shear zones in the central domain of the Cameroon Pan African Fold Belt. The tectonic evolution in the central segment of the CCSZ commenced

with ductile deformation and terminated with brittle deformation (Nguiessi et al., 1997). This is a classical feature of brittle-ductile shear zones (Passchier et al., 1993; Suh and Dada, 1997; Passchier and Trouw, 1998), although macroscopically brittle deformation predates a ductile event in certain shear zones (Imber et al., 2001).

The acquired new structural data and results show that the central Cameroon shear zone acts as a transpressive sinistral shear zone in the Magba area. On a regional scale, Neoproterozoic sinistral transpression is well documented in Keraf suture in NE Sudan (Mohamed et al., 1998). The transpressive tectonic regime has been proposed for the Kimbi area, northwestern Cameroon by Ganno et al. (2010) and also for Pan-African Trans-Saharan belt of eastern Nigeria (Ferré et al., 2002).

***Conditions of emplacement of Magba rocks***

The presence of curved foliation in mylonites and orthogneisses, euhedral to sub-hedral porphyroclasts in the crushed matrix and other rolling structures indicate the syn-tectonic emplacement of the rock. The coexistence of the S, W, M and U type of folds with axes parallel to the foliation in Mbakop migmatites, mantled feldspar porphyroclasts in Magba mylonites represents the sinistral shear sense associated with a simple shear component. Other important kinematic indicators such as S-C fabric, shear bands, sinistral asymmetric folding and sub-horizontal stretching lineations also confirm the existence of major sinistral strike-slip movement along the Magba shear zone. Further, the microstructural evidences like "σ" and "δ" porphyroclasts with stair stepping structure also corroborate the sinistral strike slip movement. "δ" type of porphyroclasts giving the dextral shear sense have been described by Njonfang et al. (2006) on the Waka'a mylonite of Foumban-Bankim shear zone (corresponds to the same mega shear zone (CCSZ) with Magba shear zone). This difference in sense of rotation of shear indicators is probably due to the complexity of Cameroon Central shear zone kinematics.

The presence of refolding in different scales, thrusts, strike-slip shears and evidence of E-W to NW-SE shortening clearly suggest that horizontal compression, rather than vertical tectonics, was the dominant stress regime during the deformation of Magba rocks (Fig. 12). The brittle-ductile behaviour of feldspars, neocrystallisation of sericite in metagabbro and mylonites, presence of the deformation lamellae, flame perthite, myrmekitic intergrowth at the margins of K-feldspar porphyroclasts, and the conversion of feldspars into sericites; all these features indicate that the Magba shear zone developed during medium-grade metamorphic conditions (450-600°C) (Passchier and Trouw, 2005).

Based on the granite and quartz flow laws (Rutter and Neumann, 1995), the intra-crystalline plasticity in quartz components of granites can be expected in the presence of melts under appropriate differential stresses (>1 MPa) and high temperatures. This is also evident by the coexistence of plastic and magmatic deformations on the mineral scale (quartz, feldspar, hornblende, sphene) which indicates recrystallization under high temperature in orthogneisses. Furthermore, the parallelism between the magmatic state and the solid state deformation fabrics in the granites, the presence of both pre-full crystallization fabric (pfc) and mylonitic fabrics and their mutual parallelism coupled with its confinement within the shear zone and linearity in disposition, suggest syntectonic emplacement of the granites.

The granites could have utilized the earlier gently dipping $D_3$ (subvertical and subhorizontal) shear zones and axial planes ($F_3$ and $C_3$) (Fig. 12b) as conduits for intrusion, followed by the emplacement of mafic dykes and gabbros during the late $D_3$ deformation phase (Fig. 12b). The sense of movement at the top of the granite sheet is consistently towards the west. In Magba area jogs (several meters long) of granite are separated by sections where granites have been sheared completely. This could be indicative of strike-slip dilatancy pumping as described by D'Lemos et al. (1992) and Brown (1994). The magma would have been channeled during $D_3$ tectonic event along the active shear zones; which acted as feeder channels at mid-crustal levels and were emplaced as one or more sheets at different places along the suitable sub-horizontal surfaces within the gneissic host rocks (Fig.12a and 12b). Variations in the rheological properties of rocks surrounding the shear zones create fragile, dilational, low-mean-pressure triple points into which ascending magmas were entered and crystallised as sheets within permeable shears giving rise to plutons (Olavis et al., 1996).

The rocks were subsequently deformed in magmatic and sub-magmatic states as the K-feldspar phenocrysts in the granite sheets were imbricated (Fig.5a) in response to tectonic movements along the sub-horizontal shear zones. The solid state deformation in the granites was mainly confined along the brittle faults.The passage of magma is driven by alternating compression and dilatation within the anastomising shear zone. The extensional parts of the shear zones are filled with magma which during the subsequent compression is squeezed upwards into overlying dilatant cavities in the zone.

The tectonic control and the timing of the intrusion of the granite to the early $F_3$ folding suggest that an NE-SW trending shearing and a NW-SE directed compression acted contemporaneously during the emplacement of the Magba granite (Fig.12a). This defines a transpressional tectonic regime during the $D_3$, with the combination of sub-vertical and sub-horizontal shears in the mid-crust. Fractures might have caused the decompression melting of deeper source (mantle) resulting in the generation of small quantities of mafic magma which transported through the same fracture channel that helped the ascent of felsic magma, hence these mafic magmas are emplaced within the early crystalized granites in the form of mafic dykes and gabbros (Fig. 12b).

All these observations propose that the kinematic emplacement of granitic plutons controlled by active shear zones as seen in Magba area is not a localized phenomenon, but could be a widespread regional feature in the Pan-Africa from western to eastern Cameroon, eastern Nigeria and NE Brazil, and pluton scale detailed structural studies in future will bring out these features.

## CONCLUSIONS

The results of this study can be summarized as follows.

1) The study area consists of six rock types variably affected by deformation: (i) Coarse- to fine- grained granites with mainly porphyritic texture, (ii) Migmatites with grano-porphyroblastic texture, (iii) Orthogneisses exhibiting porphyroblastic to grano-lepidoporphyroblastic textures, (iv) Metagabbro with granoblastic texture, (v) mafic dykes with cataclastic texture, and (vi) Proto-mylonites, mylonites and ultramylonites showing granoclastic, ocelar mylonitic and cataclastic textures respectively.
2) The rocks of Magba area experienced four stages of deformation: (i) The first stage ($D_1$), characterized by foliation ($S_1$), corresponded to tangential movements; (ii) the second ($D_2$) overprinted by $D_3$ phase, is a heterogeneous simple shear in dextral transpressive regime; (iii) the $D_3$ tectonic phase is the main tectonic event, marked by sinistral transpressive movements. It is a shearing phase with a NE-SW direction and also the phase of superposed folding; (iv) $D_4$ stage is a brittle phase which at the regional scale, is contemporaneous with the Central Cameroon shear zone. The brittle deformation is younger than the foliations and the region experienced a ductile to brittle transition deformation.
3) Kinematic indicators, petrographic characteristics and polyphase deformation indicate the primary magmatic intrusive origin for Magba granites, rather than due to the remobilization of adjacent gneisses.A possible intrusive mechanism for the Magba granites could have been a strike-slip dilatancy pumping along the sub-

vertical and sub-horizontal shear zones in a regional transpressional setting.

*Acknowledgements:* We thank the Director, CSIR-NGRI for permitting to publish this work. The data presented here forms the Ntieche's Ph.D thesis, and acknowledges the CSIR-TWAS fellowship to carry out this work.

**References**

Basseka, C.A., Shandini, Y., and Tadjou, J.M. (2011) Sub-surface structural mapping using gravity data of the northern edge of the Congo Craton, South Cameroon: Geofizika, v.28(2), pp.229-245.

Bell, T.H. (1981) Foliation development—the contribution, geometry and significance of progressive, bulk, inhomogeneous shortening. Tectonophys., v.75, pp.263-296.

Blenkinsop, T.G. (1989) Deformation Microstructures and Mechanisms in Minerals and Rocks. Kluwer Academic Publishers

Blumenfeld, P. (1983) Le "tuilage des mégacristaux", un critére d'écoulement rotationnel pour les fluidalités des roches magmatiques. Application au granite de Barbey-Séroux (Vosges, France). Bull. Soc. géol. Fr. 7 Ser. XXV, pp.309-318.

Blumenfeld, P. and Bouchez, J.-L. (1988) Shear criteria in granite and migmatite deformed in the magmatic and solid states. Jour. Struct. Geol., v.10, pp.361-372.

Brown, M. (1994) The generation, segregation, ascent and emplacement of granite magma: the migmatite- to-crustally-derived granite connection in thickened orogens. Earth Sci. Rev. v.36, pp.83-130.

Burg, J.P., Corsini, M., Diop, C., Maurin, J.C. (1993) Structure et cinématique du Sud de la chaîne des Mauritanides: un système de nappe tégumentaire varisque. C. R. Acad. Sci., v.317, pp.697-703.

Cobbold, P.R., Gapais, D., Rossello, E.A. (1991) Partitioning of transpressive motions within a sigmoidal fold belt: the Variscan Sierras Australes, Argentina. Jour. Struct. Geol., v.13, pp.743-758.

Dabo, M., Gueye, M., Ngom, P.M., Diagne, M. (2008) Orogen-parallel tectonic transport: transpression and strain partitioning in the Mauritanides of NE Senegal. *In:* Ennih, N & Liégeois, JP. (eds) The Boundaries of West African Craton. Geol. Soc. London, Spec. Publ., v.297, pp.483-497.

Den Tex, E. (1969) Origin of ultramafic rocks, their tectonic setting and history. Tectonophys., v.7, pp.457-488.

D'Lemos, R.S., Brown, M. & Strachan, R.A. (1992) Granite magma generation, ascent and emplacement within a transpressional orogen. Jour. Geol. Soc. London, v.149, pp.287-490.

Ferré, E., Gleizes,G., Caby, R. (2002) Obliques convergent tectonics and granite emplacement in the Trans-Saharian belt of Eastern Nigeria: a Synthesis. Precambrian Res., v.114, pp.199-219.

Feybesse, J.L., Johan, V., Triboulet, C., Guerrot, C., Mayaga- Mikolo, F., Bouchot, V., and Eko N'dong, J. (1998) The West Central African belt: A model of 2.5–2.0 Ga accretion and two-phase orogenic evolution: Precambrian Res., v.87, pp.161-216.

Ganno, S., Nzenti, J., Ngnotue, T., Kankeu, B., Kouankap, N. G. D.(2010)Polyphase deformation and evidence for transpressive tectonics in the Kimbi area, Northwestern Cameroon Pan-African fold belt. Jour. Geol. Min. Res., v.2(1), pp.1-015.

Goldstein, G.A. (1988) Factors affecting kinematic interpretation of asymmetric boudinage in shear zones. Jour. Struct. Geol., v.10, pp.707-715.

Ghosh, S.K. and Sengupta, S. (1987).Progressive evolution of structures in a ductile shear zone. Jour. Struct. Geol., v. 9, pp.277-288.

Hancock, S. L., and Rutland, W. R. (1984) Tectonics of the early Proterozoic geosuture: The Halls Creek Orogenic Sub-Province, Northern Australia. Jour. Geodynamics, v.1, pp.387-432.

Hanmer, S. (1986) Asymmetrical pull-aparts and foliation fish as kinematic indicadors. Jour. Struct. Geol., v.8, pp.111-122.

Ildefonse, B., Sokoutis, D. and Mancktelow, N.S. (1992a) Mechanical interactions between rigid particles in a deforming ductile matrix. Analogue experiments in simple shear flow. Jour. Struct. Geol., v.14, pp.1253-1266.

Ildefonse, B., Launeau, P., Bouchez, J.-L.and Fernandez, A. (1992b) Effect of mechanical interactions on the development of shape preferred orientations: a two-dimensional experimental approach. Jour. Struct. Geol., v.14, pp.73-83.

Imber, J., Holdsworth, R.E., Butler, C.A., Strachan, R.A. (2001) A reappraisal of the Sibson-Scholz fault zone model: the nature of frictional to viscous ("brittle-ductile") transition along a long-lived crustal scale fault, Outer Hebrides Scotland. Tectonics, v.20, pp.601-624.

Jones, R.R. and Tanner, P.W.G. (1995) Strain partitioning in transpression zones. Jour. Struct. Geol., v.17, pp.793-802.

Kankeu, B., Greiling, R.O., Nzenti, J.P. (2009) Pan-African strike-slip tectonics in eastern Cameroon-Magnetic fabrics (AMS) and structure in the Lom basin and its gneissic basement (Bétare-Oya area). Precambrian Res., v.17(3-4), pp.258-272.

Lerouge, C., Cocherie, A., Toteu, S.F., Penaye, J., Milési, J.P., Tchameni, R., Nsifa, E.N., Mark Fanning, C., and Deloule, E. (2006) Shrimp U–Pb zircon age evidence for Paleoproterozoic sedimentation and 2.05 Ga syntectonic plutonismin the Nyong Group, South-Western Cameroon: Consequences for the Eburnean-Transamazonian belt of NE Brazil and Central Africa. Jour. African Earth Sci., v.44, pp.413–427.

Lister, G. S. & Snoke, A. W. (1984) S-C Mylonites. Jour. Struct. Geol., v.6, pp.617-638.

Miller, R. B. & Paterson, S. R. (1994) The transition from magmatic to high-temperature solid-state deformation: implications from the Mount Stuart batholith, Washington. Jour. Struct. Geol., v.16, pp.853-866.

Mohamed, G., Abdelsalam, Robert, J., Stern, P. C., Elfadil, M., Elfaki, B.E., Fathelrahman, M. and Ibrahim (1998) The Neoproterozoic Keraf Suture in NE Sudan: Sinistral Transpression along the Eastern Margin of West Gondwana. Jour. Geol., v.106, pp.133-147.

Moreau, C., Regnoult, J.M., Deruelle, B., Robineau, B. (1987) A new tectonic model for the Cameroon Line, Central Africa. Tectonophys. v.139, pp.317-334.

Mvondo, H., Owona, S., Mvondo, O.J., Essono, J. (2007) Tectonic evolution of the Yaoundé segment of the Neoproterozoic Central African Orogenic Belt in Southern Cameroon. Can. Jour. Earth Sci., v.44, pp.433-444.

Nédélec, A., Nsifa, E.N., and Martin, H. (1990) Major and trace element geochemistry of the Archaean Ntem plutonic complex (south Cameroon): Petrogenesis and crustal evolution: Precambrian Res., v.47, pp.35–50.

Ngako, V., Affaton, P., Nnange, J.M., Njanko, T. (2003) Pan-African tectonic evolution in central and southern Cameroon: transpression and transtention during sinsistral shear movements. Jour. African Earth Sci., v.36, pp.207-214.

Ngako, V., Affaton, P., Njonfang, E.(2008) Pan-African tectonics in northwestern Cameroon: Implication for the history of western Gondwana. Gondwana Res., v.14, pp.509-522.

Nguiessi, T.C., Nzenti, J.P., Nsifa, E.N., Tempier, P., Tchoua, F.M. (1997) Les granitoïdes calco-alcalins, syn-cisaillement de Bandja dans la Chaîne Panafricaine Nord-Equatoriale au Cameroun. C. R. Acad. Sci., v.325, pp.95-101.

Njonfang, E., Ngako, V., Kwekam, M., Affaton, P. (2006) Les orthogneiss calcoal-calins de Foumban-Bankim : témoins d'une zone interne de marge activepanafricaine en cisaillement. Comptes Rendus Géosciences, v.338, pp.606-616

Njonfang, E., Ngako, V., Moreau, C., Affaton, P., Diot, E. (2008) Restraining bends in high temperature shear zones: the "Central Cameroon Shear Zone", Central Africa. Jour. African Earth Sci. v.52, pp.9-20.

Ntiéche, B. (2009) Etude pétrographique et géo-environnementale des granitoïdes de la zone de Magba Ouest Cameroun. DEA Univ. Yaoundé I. p.53.

Nzenti, J.P., Barbey, P., Macaudiere, J., Soba, D. (1988) Origin and evolution of the late Precambrian high-grade Yaoundé gneisses (Cameroon). Precambrian Res., v.38, pp.91-109.

Olavi, S., Ehlers,C., and Lindroos, A. (1996) Structural features and emplacement of the late Svecofennian Perniö granite sheet in southern Finland. Bull. Geol. Soc. Finland, no.68, Part 2, pp.5-17.

Passchier, C.W., Ten Brink, C.E., Bons, P.D., Sokoutis, D. (1993) Delta objects as a gauge for stress sensitivity of strain rate in mylonites. Earth Planet. Sci. Lett., v.120, pp.239-245.

Passchier, C.W. and Trouw, R.A.J. (1996) Microtectonics. Springer-Verlag, Berlin Heidelberg New York.

Passchier, C.W. and Trouw, R.A.J. (1998) Microtectonics. Springer, Berlin, pp.1-289.

Passchier, C.W. and Trouw, R.A.J. (2005) Micro-tectonics, 2nd Ed, Springer, Germany.

Paterson, S.R., Vernon, R.H. and Tobisch, O.T. (1989) A review of criteria for

the identification of magmatic and tectonic foliations in granitoids. Jour. Struct. Geol. v.11, pp.349-363.

Penaye, J., Toteu, S.F., Tchameni, R., Van Schmus, W.R., Tchakounté, J., Ganwa, A., Minyem, D., and Nsifa, E.N. (2004) The 2.1 Ga West Central African Belt in Cameroon: Extension and evolution: Jour. African Earth Sci., v.39, pp.159–164.

Ragan, D.M. (1973) Structural geology: an introduction to geometrical techniques. 2nd edition, John Wiley and Sons, New York, pp.1-208.

Rutter, E.H. and Neumann, D.H.K. (1995) Experimental deformation of partially molten Westerly granite under fluid-absent conditions, with implications for the extraction of granitic magmas. Jour. Geophys. Res., v.100, pp.15697-15715.

Shang, C.K., Satir, M., Siebel, W., Nsifa, E.N., Taubald, H., Liégeois, J.P., and Tchoua, F.M. (2004) TTG magmatism in the Congo craton; a view from major and trace element geochemistry, Rb–Sr and Sm–Nd systematics: Case of the Sangmelima region, Ntem complex, southern Cameroon: Jour. African Earth Sci., v.40, pp.61-79.

Shang, C., Satir, M., Nsifa, E., Liégeois, J.P., Siebel, W. and Taubald, H. (2007) Archaean high-K granitoids produced by remelting of earlier TonaliteTrondhjemite–Granodiorite (TTG) in the Sangmelima region of the Ntem complex of the Congo craton, southern Cameroon: Internat. Jour. Earth Sci., v.96, pp.817-841.

Suh, C.E., Dada, S.S. (1997) Fault rocks and differential reactivity of minerals in the Kanawa Violaine uraniferous vein, NE Nigeria. Jour. Struct. Geol., v.19, pp.1037-1044.

Suh, C.E., Cabral, A.R., Shemang, E.M., Mbinkar, L., and Mboudou, G.G.M. (2008) Two contrasting iron deposits in the Precambrian mineral belt of Cameroon, West Africa: Exploration and Mining Geol., v.17, pp.197–207.

Tanko, N.E.L., Nzenti, J.P., Njanko, T., Kapajika, B., and Nédélec, A. (2005) New U–Pb zircon ages from Tonga (Cameroon): Coexisting Eburnean-Transamazonian (2.1 Ga) and Pan-African (0.6 Ga) imprints: Comptes Rendus Geosciences, v.337, pp.551-562.

Tchameni, R., Mezger, K., Nsifa, N.E., and Pouclet, A. (2001) Crustal origin of Early Proterozoic syenites in the Congo Craton (Ntem Complex), South Cameroon: Lithos, v.57, pp.23-42.

Tcheumenak, K.J., Njanko, T., Kwekam, M., Naba, S., Bella Nke, B.E., Yakeu Sandjo, A.F., Fozing, E.M., Njonfang, E. (2014) Kinematic evolution of the Fodjomekwet-Fotouni Shear Zone (West-Cameroon): Implications for emplacement of the Fomopea and Bandja plutons: Jour. African Earth Sci., v.99, pp.261–275.

Tikoff, B., De Saint Blanquatt, M. (1997) Transpressional shearing and strike-slip partitioning in the late Cretaceous Sierra Nevada magmatic arc, California. Tectonics, v.16, pp.442-459.

Toteu, S.F., Van Schmus, W.R., Penaye, J., and Nyobé, J.B.(1994) U-Pb and Sm-N edvidence for Eburnian and Pan-African high-grade metamorphism in cratonic rocks of southernCameroon: Precambrian Res., v.67, pp.321–347.

Toteu, S.F., Van Schmus, W.R., Penaye, J. and Michard, A. (2001) New U–Pb and Sm–Nd data from north-central Cameroon and its bearing on the pre-Pan African history of central Africa: Precambrian Res., v.108, pp.45-73.

Toteu, S.F., Penaye, J., and Djomani, Y.P. (2004) Geodynamic evolution of the Pan-African belt in central Africa with special reference to Cameroon: Canadian Jour. Earth Sci., v.41, p.73-85.

Toteu, S.F., Penaye, J., Deloule, E., Van Schmus, W.R., and Tchameni, R. (2006a) Diachronous evolution of volcanosedimentary basins north of the Congo craton: Insights from U–Pb ion microprobe dating of zircons from the Poli, Lom and Yaoundé Groups (Cameroon): Jour. African Earth Sci., v.44, pp.428–442.

Toteu, S.F., Van Schmus, W.R., and Penaye, J. (2006b) The Precambrian of Central Africa: Summary and perspectives: Jour. African Earth Sci., v.44, pp.vii–x.

Van Schmus, W.R., Oliveira, E.P., Da Silva Filho, A.F., Toteu, S.F., Penaye, J., and Guimaraes, I.P. (2008) Proterozoic links between the Borborema Province, NE Brazil, and the Central African Fold Belt: Geol. Soc. London, Spec. Publ., v.294(1), pp.69-99.

*(Received: 25 April 2015; Revised form accepted: 5 February 2016)*